0026-895X/08/7304-1225–1234$20.00
MOLECULAR PHARMACOLOGY
Vol. 73, No. 4
42663/3314892
Mol Pharmacol 73:1225–1234, 2008
Printed in U.S.A.

Activation of TRPA1 by Farnesyl Thiosalicylic Acid

Michael Maher, Hong Ao, Tue Banke, Nadia Nasser, Nyan-Tsz Wu, J. Guy Breitenbucher, Sandra R. Chaplan, and Alan D. Wickenden

Johnson & Johnson Pharmaceutical Research & Development, L.L.C., San Diego, California

Received October 15, 2007; accepted December 31, 2007

ABSTRACT

The nonselective cation channel TRPA1 (ANKTM1, p120) is a potential mediator of pain, and selective pharmacological modulation of this channel may be analgesic. Although several TRPA1 activators exist, these tend to be either reactive or of low potency and/or selectivity. The aim of the present study, therefore, was to identify novel TRPA1 agonists. Using a combination of calcium fluorescent assays and whole-cell electrophysiology, we discovered several compounds that possess potent, selective TRPA1-activating activity, including several lipid compounds (farnesyl thiosalicylic acid, farnesyl thioacetic acid, 15-deoxy-$\Delta^{12,14}$-prostaglandin J_2, and 5,8,11,14-eicosatetraynoic acid), and two marketed drugs: disulfiram (Antabuse; a compound used in the treatment of alcohol abuse) and the antifungal agent chlordantoin. Farnesyl thiosalicylic acid activates the channel in excised patches and in the absence of calcium. Furthermore, using a quadruple TRPA1 mutant, we show that the mechanism of action of farnesyl thiosalicylic acid differs from that of the reactive electrophilic reagent allylisothiocyanate. As a TRPA1 agonist with a potentially novel mechanism of action, farnesyl thiosalicylic acid may be useful in the study of TRPA1 channels.

TRPA1 (ANKTM1, p120) is a nonselective cation channel that belongs to the transient receptor potential (TRP) superfamily. To date, TRPA1 is the only member of the TRPA subfamily in mammals. TRPA1 was first identified as a transformation-sensitive mRNA in cultured human lung fibroblasts (Jaquemar et al., 1999). Subsequent studies indicated that TRPA1 was also highly expressed in sensory neurons of the dorsal root, trigeminal, and nodose ganglia, and in hair cells of the inner ear (Story et al., 2003; Corey et al., 2004; Nagata et al., 2005; Diogenes et al., 2007). Furthermore, TRPA1 expression seems to be restricted to sensory neurons, with little or no expression in nonsensory neurons or in a variety of organs and tissues (Story et al., 2003; Nagata et al., 2005), although recent evidence indicates that TRPA1 expression may be more widespread than originally thought (Stokes et al., 2006). In sensory neurons, TRPA1 expression is most prevalent in small-diameter neurons where it colocalizes with markers of peptidergic nociceptors such as TRPV1, calcitonin gene-related peptide, and substance P (Story et al., 2003; Bautista et al., 2005; Nagata et al., 2005; Diogenes et al., 2007).

The finding that TRPA1 is expressed in small-diameter nociceptors has led to the suggestion that this channel may be involved in pain sensation. Indeed, a number of additional observations support this suggestion. For example, TRPA1 expression can be increased by inflammatory mediators such as nerve growth factor (Diogenes et al., 2007) and after nerve injury or inflammation (Obata et al., 2005; Frederick et al., 2007). Bradykinin, a potent algogenic peptide released at sites of injury and inflammation, can activate TRPA1 via G protein-coupled bradykinin B2 receptors (Bandell et al., 2004). In addition, TRPA1 can be activated by a range of pungent or irritant compounds that can elicit pain in animals and humans, such as mustard oil [allyl isothiocyanate (AITC)], cinnamaldehyde, acrolein, allicin, and formalin (Bandell et al., 2004; Namer et al., 2005; Bautista et al., 2006; Fujita et al., 2007; McNamara et al., 2007). TRPA1 may also be activated by noxious cold (<17°C), although this remains controversial (Bandell et al., 2004; Jordt et al., 2004; Nagata et al., 2005). In behavioral studies, intrathecal TRPA1 antisense oligodeoxynucleotide suppressed inflammation and nerve injury-in-

Article, publication date, and citation information can be found at http://molpharm.aspetjournals.org.
doi:10.1124/mol.107.042663.

ABBREVIATIONS: TRP, transient receptor potential; TRPV, transient receptor potential vanilloid; AITC, allyl isothiocyanate; URB957, 3′-carbamoylbiphenyl-3-yl cyclohexylcarbamate; WIN55212-2, (*R*)-(+)-[2,3-dihydro-5-methyl-3-(4-morpholinylmethyl) pyrrolo-[1,2,3-*d*,*e*]-1,4-benzoxazin-6-yl]-1-naphthalenyl-methanone; FTS, farnesyl thiosalicylic acid; FTA, farnesyl thioacetic acid; 15d-PGJ_2, 15-deoxy-$\Delta^{12,14}$-prostaglandin J_2; ETYA, 5,8,11,14-eicosatetraynoic acid; HEK, human embryonic kidney; FLIPR, fluorometric imaging plate reader; RR, ruthenium red; 4αPDD, 4-α-phorbol-12,13-didecanoate; DRG, dorsal root ganglion; DMSO, dimethyl sulfoxide; CHO, Chinese hamster ovary; WT, wild type; PG, prostaglandin.

duced cold allodynia (Obata et al., 2005). Moreover, mustard oil-induced pain behaviors and bradykinin-induced acute pain and hyperalgesia are abolished in TRPA1−/− mice (Bautista et al., 2006; Kwan et al., 2006). Although these findings support a role for TRPA1 in some forms of pain sensation, its exact role is not fully understood. Despite deficits in bradykinin and mustard oil-induced pain, TRPA1 null mice show no deficit in either complete Freund's adjuvant-induced thermal hyperalgesia or nerve injury-induced mechanical allodynia (Bautista et al., 2006; Kwan et al., 2006).

Further studies to explore the role of TRPA1 would be greatly facilitated by the availability of potent, selective TRPA1 modulators. Although several TRPA1 activators exist, these tend to be either reactive or of low potency and or selectivity. For example, agents such as mustard oil (AITC), cinnamaldehyde, allicin, and acrolein are highly reactive electrophiles that activate TRPA1 by reversible covalent modification of cysteine and lysine residues in the N terminus of the channel (Hinman et al., 2006; Macpherson et al., 2007). The reactive nature of these compounds makes it highly likely that they could modify other proteins in addition to TRPA1. Furthermore, they are not suitable for use in high-throughput screening assays, because they have the potential to react with other assay reagents. Other nonreactive agents, such as URB597 (Niforatos et al., 2007), methyl *p*-hydroxybenzoate and related compounds (Fujita et al., 2007), WIN55212-2 (Jeske et al., 2006), and Δ^9-tetrahydrocannabinol (Jordt et al., 2004), are of questionable value as pharmacological tools because of their low potency and/or poor selectivity. We therefore set out to identify novel TRPA1 agonists. Using a combination of calcium fluorescent assays and whole-cell electrophysiology, we have identified several compounds that possess potent, selective TRPA1-activating activity, including several lipid compounds, such as farnesyl thiosalicylic acid (FTS), farnesyl thioacetic acid (FTA), 15-deoxy-$\Delta^{12,14}$-prostaglandin J2 (15d-PGJ_2), and 5,8,11,14-eicosatetraynoic acid (ETYA), along with disulfiram (Antabuse; a compound used in the treatment of alcohol abuse) and the antifungal agent chlordantoin. Furthermore, using a quadruple TRPA1 mutant, we show that the mechanism of action of FTS differs from that of AITC. Agents such as FTS may be useful in the study of TRPA1 channel regulation.

Materials and Methods

Plasmid Constructs and Cell Lines. Human TRPA1 (sequence identical to accession no. NM_007332.1) was cloned into pcDNA4/TO. CHO-TREx cells (Invitrogen, Carlsbad, CA) were stably transfected with pcDNA4/TO-TRPA1 using standard techniques to generate a clonal cell line that expressed human TRPA1 in a tetracycline-inducible manner. The culture medium was Ham's F-12 supplemented with 10% fetal bovine serum, 2 mM L-glutamine, 5 μg/ml blasticidin, and 200 μg/ml zeocin. The mustard oil-insensitive TRPA1 quadruple mutant (TRPA1-M4; Hinman et al., 2006) containing C621S, C641S, C665S, and K710R (numbering according to NP-015628.1) was prepared by site-directed mutagenesis according to standard methodology. TRPA1-M4 was transiently transfected into HEK293 using Lipofectamine 2000 (Invitrogen). For electrophysiological experiments, cells were cotransfected with truncated CD4 (pMACs 4.1; Miltenyi Biotec GmbH, Bergisch Gladbach, Germany). Assays were performed 48 h after transfection.

Clonal cell lines stably expressing rat TRPV2 (accession no. BC089215; Neeper et al., 2007), human TRPV4 (accession no. NM_021625), and canine TRPM8 (accession no. DQ273165; Liu et al., 2006) were prepared by liposomal transfection in HEK293 cells. Cells were cultured in Dulbecco's modified Eagle's medium supplemented with 10% fetal bovine serum. The media were also supplemented with the antibiotic selection marker G-418 (Geneticin; Invitrogen).

Calcium Fluorescence. For all cell types, intracellular Ca^{2+} concentrations were monitored using FLIPR (Molecular Devices, Sunnyvale, CA). Cells were seeded in black-walled clear-bottomed 96-well plates at a density of 50,000 cells/well, and they were cultured overnight at 37°C with 5% CO_2 in culture medium supplemented with 1 μg/ml tetracycline if appropriate. On the day of the experiment, cells were washed three times with HEPES-buffered saline (137 mM NaCl, 0.5 mM $MgCl_2$, 2 mM KCl, 5 mM dextrose, 2 mM $CaCl_2$, and 10 mM HEPES, pH 7.4). Cells were then loaded with calcium-sensitive fluorescent dye by incubation in the presence of 4 μM Fluo-3/acetoxymethyl ester (TefLabs, Austin, TX) at room temperature in the dark for 60 min. After incubation with dye, cells were washed in assay buffer, and, if appropriate, antagonists were added at this time. After a further 30-min incubation, cells were assayed in FLIPR. Changes in fluorescence were monitored for 3 min after the addition of test agonist. Responses were normalized to the fluorescence change induced by a positive control (100 μM AITC unless otherwise noted).

The concentration of calcium in the assay buffer varied, depending on the cell line being studied. In tetracycline-induced CHO-TREx-TRPA1 cells, AITC-induced increases in calcium fluorescence could not be blocked with ruthenium red (RR) when using normal (2 mM) extracellular calcium, presumably because of high expression levels. Therefore, we reduced the extracellular calcium concentration to 20 μM, to optimize for ruthenium red block. In contrast, cells transiently transfected with the quadruple mutant TRPA1-M4 had much lower expression, necessitating the use of higher (2 mM) extracellular calcium. In experiments involving zero extracellular calcium, calcium was first removed by preincubating cells for 2 min in buffer containing zero added calcium and 1 mM EGTA. Agonists were then applied in zero calcium assay buffer.

Untransfected cells, HEK-TRPV2, HEK-TRPM8, and HEK-TRPV4 were also tested in 2 mM extracellular calcium, whereas HEK-TRPV1 was tested in 20 μM calcium. These conditions were chosen by matching the potency of known agonists to literature values. Capsaicin increased calcium fluorescence in the HEK-TRPV1 assay, with an EC_{50} value of 11 nM. 2-Aminophenyl borate activated HEK-TRPV2 in this assay, with an EC_{50} value of ~100 μM (Hu et al., 2004). 4-α-phorbol-12,13-didecanoate (4αPDD) (EC_{50} value of ~1 μM) and a hypo-osmotic stimulus (threshold ~240 mOs) activated HEK-TRPV4 (Nilius et al., 2003). Icilin activated HEK-TRPM8, with an EC_{50} value of ~100 nM (Andersson et al., 2004).

Data Analysis. Concentration-response data were normalized to positive and negative controls (specified below for the individual experiments). Concentration-response data were fitted to a Hill function using the nonlinear analysis routine in Origin 7 (OriginLab Corp., Northampton, MA). Averages of multiple measurements are reported as mean ± S.D. unless otherwise noted.

Rat DRG. The protocol for the isolation of rat dorsal root ganglia was approved by the Institutional Animal Care and Use Committee of Johnson & Johnson Pharmaceutical Research & Development, L.L.C. Adult male Sprague-Dawley rats (Harlan, Indianapolis, IN) were housed in cages with corncob bedding, with ad libitum access to chow and water. L4-L6 dorsal root ganglia were aseptically excised, washed in ice-cold Tyrode's solution (145 mM NaCl, 4 mM KCl, 1 mM $CaCl_2$, 1.2 mM $MgCl_2$, 10 mM dextrose, and 10 mM hemisodium HEPES, pH 7.3), supplemented with 50 mg/l gentamicin, and incubated in Tyrode's solution containing 2 mg/ml collagenase and 1 mg/ml protease for 45 min at 37°C with 5% CO_2. After digestion, ganglia were washed in Tyrode's solution, transferred into 1 ml of Dulbecco's modified Eagle's medium with 10% fetal bovine serum, and single cells were liberated by gentle mechanical agitation using

a disposable transfer pipette. Cells were plated on poly-D-lysine-coated coverslips, and they were maintained at 37°C.

Electrophysiology. Cells for use in electrophysiological assays were plated at low density onto glass coverslips 24 to72 h before recording, and they were maintained in appropriate media. On the day of the experiment, glass coverslips were placed in a bath on the stage of an inverted microscope, and they were perfused (approximately 1 ml/min) with extracellular solution of the following composition: 137 mM NaCl, 2 mM $CaCl_2$, 5.4 mM KCl, 1 mM $MgCl_2$, 5 mM glucose, and 10 mM HEPES, pH 7.4. In some experiments, extracellular calcium was replaced with barium. Pipettes were filled with an intracellular solution of the following composition: 40 mM KCl, 100 mM potassium fluoride, 2 mM $MgCl_2$, 10 mM EGTA, and 10 mM HEPES, pH 7.3 to 7.4, and they had a resistance of 2 to 4 MΩ. All recordings were made at room temperature (22–24°C) using a Multiclamp 700A amplifier and pClamp 9 software (Molecular Devices, Sunnyvale, CA). Transfected HEK293 cells were identified using anti-CD4-coated beads (Dynabeads; Invitrogen). Inward TRPA1 currents were measured using the whole-cell configuration of the patch-clamp technique at a holding potential of −60 mV. In some experiments, TRPA1 currents were elicited with voltage ramps from −80 to +40 mV. Current records were acquired at 2 to 5 KHz, and they were filtered at 1 to 2 KHz. Agonists were applied using an SF-77B Fast-Step Perfusion device (Warner Instruments, Hamden, CT). The liquid junction potential was calculated to be 7.1 mV at 20°C, and voltage commands were not corrected.

For inside-out patch recordings, both bath and pipette solutions contained 140 mM NaCl, 2 mM $MgCl_2$,5 mM EGTA, 7 mM sucrose, and 10 mM HEPES, pH 7.4. Pipette resistance was 2 to 4 MΩ. TRPA1 currents elicited at holding potentials between +80 and −80 mV were acquired at 10 KHz and filtered at 2 KHz (eight-pole Bessel filter, −3 dB; Frequency Devices, Haverhill, MA). Amplitude histogram plots were generated using ClampFit 9.2 (Molecular Devices). Potentials indicated are membrane potentials (i.e., potential of the inner side of the membrane relative to the outside).

Test Compounds. The identified lipid compounds were purchased from BIOMOL Research Laboratories (Plymouth Meeting, PA). Disulfiram, allyl isothiocyanate, and ruthenium red were purchased from Sigma-Aldrich (St. Louis, MO). Chlordantoin was obtained from a proprietary compound collection. Stock solutions of compounds were solubilized in DMSO at 10 to 100 mM. For potency determinations, serial dilutions of compounds were performed into extracellular solution. Solubility in saline was determined by nephelometry 30 min after the final dilution into saline. Final DMSO concentration did not exceed 0.1% in electrophysiology experiments and 0.5% in calcium fluorescence experiments. These DMSO concentrations were without effect on TRPA1 activity (data not shown).

Results

Identification of TRPA1 Agonists: Calcium Fluorescence Studies. FTS, FTA, disulfiram, chlordantoin, 5d-PGJ_2, and ETYA (structures shown in Fig. 1), along with the known TRPA1 agonist AITC, increased calcium fluorescence in CHO-TREx-TRPA1 cells. As illustrated in Fig. 2A, 25 μM AITC induced a large and sustained increase in fluorescence in TRPA1-expressing cells. In these experiments, intracellular calcium levels remained elevated for the duration of the experiment. Comparable increases were observed with 10 μM FTS (Fig. 2B). All agents increased calcium fluorescence in a concentration-dependent manner as illustrated for AITC and FTS in Fig. 2, C and D, respectively. In these experiments, increases in calcium fluorescence were normalized to the fluorescence level measured in the presence of 100 μM AITC at the end of the 3-min exposure. EC_{50} values and the maximal response relative to 100 μM AITC for all the agonists are shown in Table 1. The response to ETYA was essentially linear over the range of agonist concentrations tested, and it reached levels far larger than the saturating responses of the other agonists. As a result, the EC_{50} value and the maximal response could not be determined accurately for this compound (Table 1). In contrast to the effects observed in TRPA1-expressing cells, AITC, FTS, disulfiram, chlordantoin, and 15d-PGJ_2 exerted little or no effect in CHO-WT cells. For example, AITC had no effect in CHO-WT cells at concentrations up to 100 μM (Fig. 2, A and C), whereas FTS only induced a response in CHO-WT cells at concentrations of 50 μM or above (Fig. 2, B and D). EC_{50} values determined in CHO-WT cells are summarized in Table 1. These values show that AITC, FTS, disulfiram, chlordantoin, and 15d-PGJ_2 only exerted effects in CHO-WT cells at concentrations that were considerably higher than those required to activate TRPA1. Conversely, FTA and ETYA increased fluorescence in CHO-WT cells at concentrations that were only marginally higher than those required for TRPA1 activation (Table 1).

Several known TRP channel agonists, such as capsaicin, resiniferatoxin (TRPV1 agonists), camphor (TRPV3 agonist), 4αPDD (TRPV4 agonist), and menthol (TRPM8 agonist), were without effect in our TRPA1 calcium fluorescence assay. 2-Aminophenyl borate (a nonselective TRP channel agonist) induced a weak activation at a concentration of 200 μM (data not shown). Given that two farnesyl-containing compounds were active in our assay (i.e., FTS and FTA), we also screened several farnesyl-related compounds, including *N*-acetyl-*S*-farnesyl-L-cysteine, *N*-acetyl-*S*-geranyl-L-cysteine, *S*-farnesyl-L-cysteine methyl ester, farnesylpyrophosphate, geranylgeraniol, geranylgeranyl-pyrophosphate, α-hydroxyfarnesylphosphonic acid, and farnesylthiotriazole. All were inactive in the fluorescence assay (data not shown).

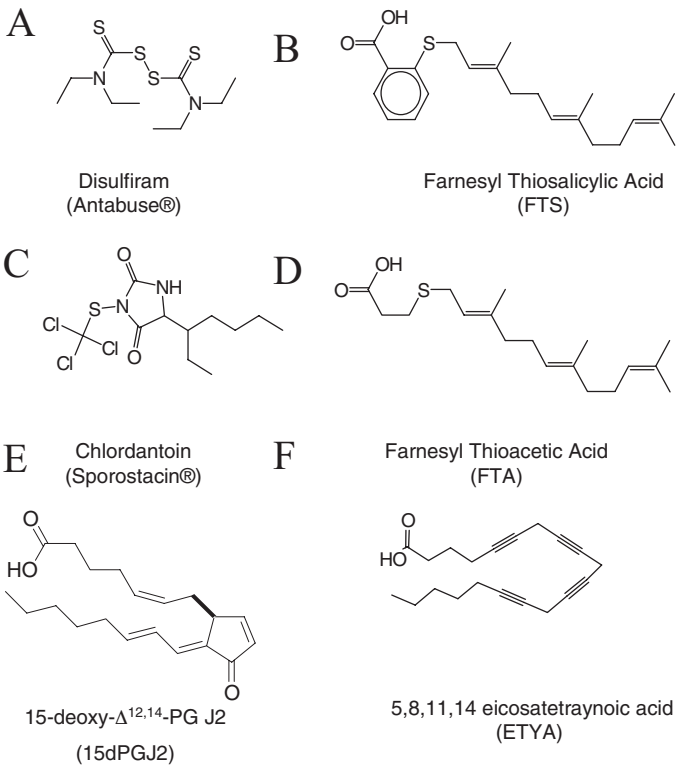

Fig. 1. Structures of novel TRPA1 agonists.

RR is a potent, membrane-impermeant antagonist of AITC-induced TRPA1 currents (Nagata et al., 2005). We investigated whether RR could inhibit the increase in fluorescence in CHO-TREx-TRPA1 induced by concentrations of each agonist that were near-saturating for TRPA1 activity but had minimal effects in CHO-WT cells. As summarized in Table 1, preincubation of cells with RR resulted in a concentration-dependent inhibition of the subsequent response to

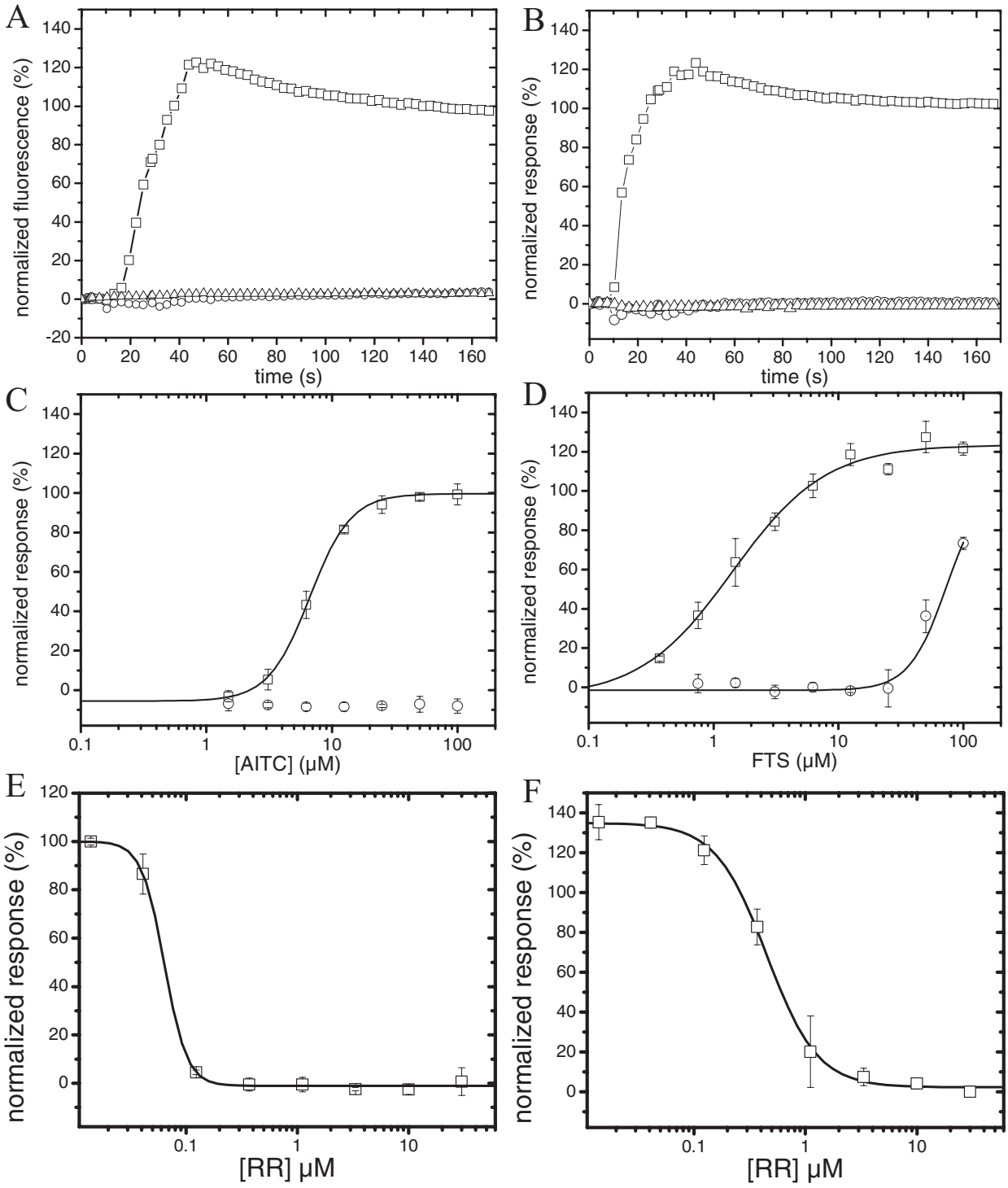

Fig. 2. Activation of TRPA1 by AITC and FTS. Top, time course of calcium-sensitive dye fluorescence after application of 25 μM AITC (A) and 10 μM FTS (B). Test compounds were added at $t = 10$ s, and the fluorescence was monitored in FLIPR. Each trace is the average of three wells. CHO-TRPA1 (□), CHO-TRPA1 without extracellular calcium (△), and untransfected CHO-WT (○). Middle, concentration-response curves for AITC (C) and FTS (D) as determined in the FLIPR assay. Symbols and error bars represent the mean ± S.D. of three independent experiments. Solid lines are Hill fits to the data. CHO-TRPA1 (□) and untransfected CHO-WT (○). Data were normalized to the response of cells expressing TRPA1 to 100 μM AITC. Bottom, inhibition of the responses to 15 μM AITC (E) and 10 μM FTS (F) by ruthenium red. The average calcium response ($n = 3$) to the addition of agonist in the presence of varying concentrations of ruthenium red were normalized to the unblocked response to 100 μM AITC. The curves are Hill fits to the data.

each agonist. RR fully blocked the response to 15 μM AITC, 10 μM FTS, 50 μM FTA, 50 μM 15d-PGJ_2, and 10 μM disulfiram, with IC_{50} values ranging from 50 to 500 nM (Table 1). Representative RR concentration-response curves for block of AITC and FTS are shown in Fig. 2, E and F, respectively. It is noteworthy that RR only partially blocked the response to 50 μM ETYA and 10 μM chlordantoin. Given the small degree of separation between activity in TRPA1-expressing cells and CHO-WT for ETYA, partial inhibition by RR is perhaps not surprising. However, the reasons for the lack of complete block for chlordantoin are not clear.

To study the requirement for calcium influx, responses to near-saturating concentrations of agonist were measured in the presence and absence of extracellular calcium. As described above, all agonists induced large and sustained increases in fluorescence in TRPA1-expressing cells. However, in the absence of extracellular calcium, the effects of the putative TRPA1 agonists were substantially reduced. This is illustrated for 25 μM AITC and 10 μM FTS in Fig. 2, A and B, respectively.

Selectivity. To assess selectivity, we screened the TRPA1 agonists identified in the present study against four related cation channels: human TRPV1, human TRPV4, canine TRPM8, and rat TRPV2. AITC was devoid of activity on all four related TRP channels at concentrations up to 100 μM (Fig. 3A). FTS also exhibited a high degree of selectivity for TRPA1 over other TRP channels (Fig. 3B). Although FTS did exert small effects at the higher concentrations (50 and 100 μM), these effects were similar in magnitude to the effects seen in untransfected cells (Fig. 2D). Likewise, disulfiram and chlordantoin exerted little or no effect on any of the four related TRP channels, at concentrations up to 100 μM (data not shown). Given the lower potency of FTA, 15d-PGJ_2 and ETYA against TRPA1, coupled with tendency of these compounds to increase calcium fluorescence in WT-HEK cells, it was difficult to fully evaluate the selectivity of these agents.

Electrophysiology. To confirm TRPA1 agonistic activity using a more direct approach, we studied the activity of selected compounds against human TRPA1 using the whole-cell patch-clamp technique.

A representative example of an agonist concentration-response experiment is shown in Fig. 4. In the example shown, FTS was applied to a TRPA1-expressing cell at a holding potential of −60 mV, starting at 0.1 μM and increasing in half-log increments to 10 μM. In this experiment, FTS did not change holding current at concentrations of 0.1 to 1 μM. At a concentration of 3 μM, FTS induced a small, sustained inward current that declined back to baseline on removal of the compound. Application of 10 μM FTS induced a large inward current that was transient. Similar observations were made in a total of three cells. Replacement of extracellular calcium with barium to limit calcium-induced desensitization (Nagata et al., 2005) did not consistently prevent the appearance of transient currents at higher agonist concentrations, particularly when currents were large, and in all experiments, a second application of 10 μM FTS resulted in the appearance of a current that was much smaller than that induced by the first application. Therefore, it was not possible to accurately determine potency in these experiments. Instead, we used the threshold concentration in the presence of 2 mM calcium (i.e., the minimal concentration required to elicit an inward current) to define the relative potency of the novel TRPA1 agonists. Threshold concentrations were 3 μM for FTS, 0.3 μM for disulfiram, and 1 μM for chlordantoin.

An example of an experiment designed to evaluate the current-voltage relationship and ruthenium red sensitivity of the drug-induced current is shown in Fig. 5. Voltage ramps of 1-s duration from −80 to +40 mV were run every 40 s during continuous recording of membrane current at a holding potential of −60 mV. In the absence of agonist, holding current was minimal and voltage ramps elicited small, linear or weakly outwardly rectifying currents. Application of 5 μM FTS induced a sustained increase in inward current (Fig. 5a), and a voltage ramp in the continued presence of FTS elicited a large current that was characterized by a negative slope conductance between −70 and −30 mV, strong outward rectification at positive potentials, a reversal potential of ~6 mV (approximately −1 mV after correction for the liquid junction potential), and a large inward tail current on repolarization to −60 mV (Fig. 5b). Application of 10 μM RR completely and reversibly inhibited the inward drug-induced current (Fig. 5A). Holding current and ramp-induced currents decayed to predrug levels on removal of FTS. Similar currents were never seen in untransfected CHO-TREx +tet cells (Fig. 5c). Disulfiram (1 μM), 3 μM chlordantoin, 50 μM FTA, and 50 μM 15d-PGJ_2 all induced similar, outwardly rectifying currents in TRPA1-expressing cells (data not shown), and the inward currents induced by disulfiram and chlordantoin were blocked by 10 μM RR (data not shown). The sensitivity

TABLE 1

Summary of the activity of TRPA1 agonists in CHO.TREx.TRPA1 and untransfected CHO.TREx cells

Maximal response is the ratio of the high-concentration response relative to the response of CHO.TREx.TRPA1 to 100 μM AITC. Values are the mean ± S.D. of nonlinear least-squares fit parameters for $n = 3$ to 5 concentration-response experiments.

Agonist	Solubility Limit	TRPA1		CHO-WT		$RRIC_{50}$
		EC_{50}	Maximal Response	EC_{50}	Maximal Response	
	μM	μM		μM		μM
AITC	100	5 ± 1	1.0	—	—	0.06 ± 0.02
FTS	100	5 ± 3	1.3 ± 0.1	41 ± 5	1.20	0.45 ± 0.05
FTA	400	90 ± 40	1.3 ± 0.1	100 ± 10	0.8 ± 0.2	0.18 ± 0.05
Disulfiram	50	3 ± 2	1.0 ± 0.2	—	—	0.08 ± 0.02
Chlordantoin	100	3 ± 1	1.1 ± 0.1	>100	N.D.	0.13 ± 0.03
15d-PGJ_2	400	18 ± 8	1.47 ± 0.08	100[a]	N.D.	0.08 ± 0.02
ETYA	25	3[a]	N.D.	20[a]	N.D.	0.18 ± 0.06

—, <20% response at the highest concentration tested; N.D., not determined.

[a] Could not be fit accurately with a Hill function. Instead of an EC_{50} value, the threshold concentration (i.e., the average concentration required to increase the normalized response by 20%) is provided for this compound.

of FTA- and 15d-PGJ_2-induced currents to RR block was not studied.

TRPA1 channels are likely regulated by a variety of intracellular second messengers, including calcium (Jordt et al., 2004; Doerner et al., 2007; Zurborg et al., 2007) and other products of phospholipase C activation (Bandell et al., 2004). To determine whether the mechanism of action of FTS involved cytosolic factors, we studied the effects of this compound on TRPA1 activity in excised inside-out membrane patches from CHO-TREx-TRPA1 cells. In these experiments, the intracellular side of the membrane faces the recording solution, allowing complete and rapid removal of the normal intracellular milieu. In addition, the pipette and bath solutions used in these experiments were identical calcium-free solutions. As indicated in Fig. 6, TRPA1 channel openings were rare in the absence of FTS. Single channel openings became more frequent shortly after exposure of the patch to 10 μM FTS via the intracellular (bath) solution, especially at positive membrane potentials, and multiple openings became apparent on continued exposure to FTS (Fig. 6A). At positive membrane potentials, Gaussian fits of single channel amplitudes were 7.2 and 5.1 pA at +80 and +60 mV, respectively (Fig. 6B), corresponding to single channel slope conductances of 90 and 85 pS (Fig. 6C). Single channel amplitudes at negative membrane potentials were typically smaller (−6.7 and −4.9 pA at −80 and −60 mV, respectively, corresponding to a single channel slope conductance of 84 and 82 pS) (Fig. 6B) (see also Kim and Cavanaugh, 2007). These findings are similar to those reported previously for mustard oil acting on single human TRPA1 channels (~90 pS; Macpherson et al., 2007; Kim and Cavanaugh, 2007). On average, single

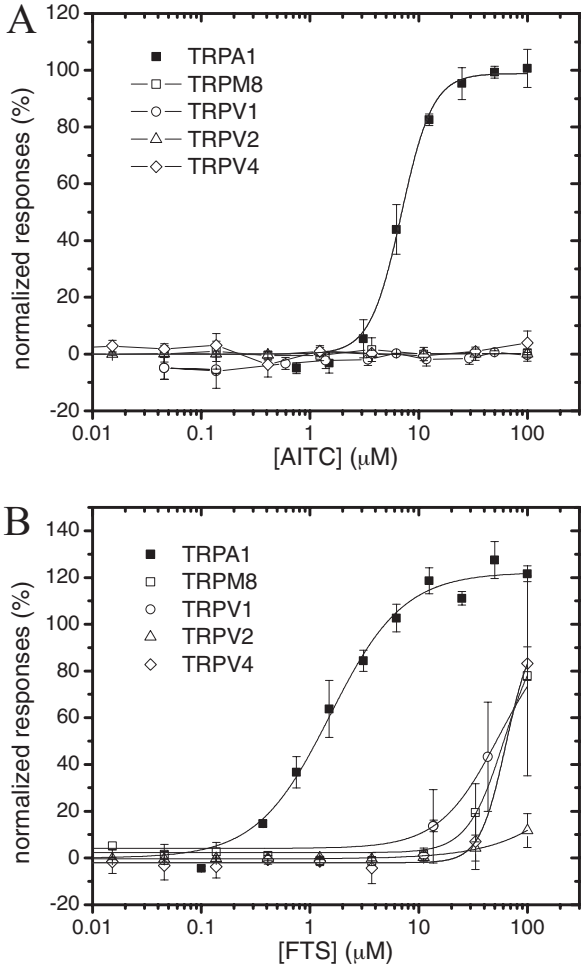

Fig. 3. TRP channel selectivity of AITC and FTS. Concentration-response curves for AITC (A) and FTS (B) against TRPA1 (■), TRPM8 (□), TRPV1 (○), TRPV2 (△), and TRPV4 (◇) as determined in the FLIPR assay. Symbols and error bars represent the mean ± S.D. of the response of three independent experiments. Solid lines are Hill fits to the data. Data were normalized to 100 μM AITC (TRPA1), 150 nM capsaicin (TRPV1), 100 nM icilin (TRPM8), 300 μM 2-aminophenyl borate (TRPV2), or 10 μM 4αPDD (TRPV4).

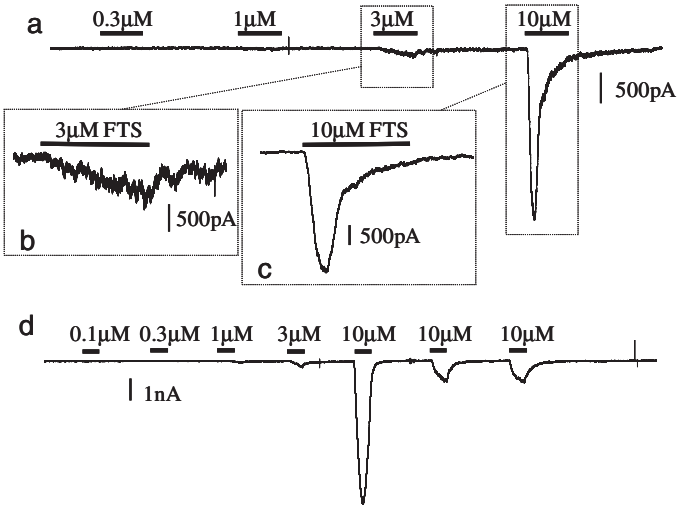

Fig. 4. Representative whole-cell patch-clamp recordings from TRPA1-expressing cells. a, the cell was held at −60 mV, and increasing concentrations of FTS were applied. The threshold concentration of FTS for TRPA1 activation was ~3 μM (b) and higher concentrations produced large, desensitizing currents (c). Desensitization to FTS was also observed when extracellular calcium was replaced with barium (d). Horizontal bars, 10 s.

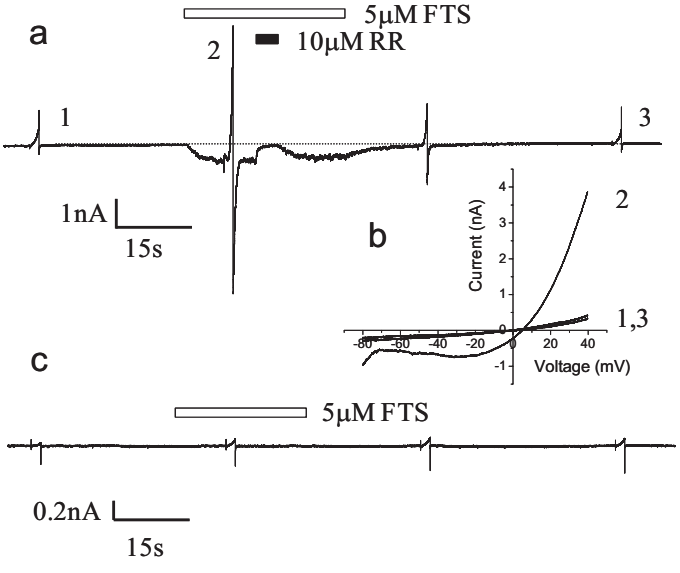

Fig. 5. FTS induces an outwardly rectifying current in CHO-TREx-TRPA1. Voltage ramps were applied to a CHO.TRPA1 cell in whole-cell mode, with a holding potential of −60 mV between ramps. a, application of 5 μM FTS rapidly activated an inward current that was blocked by 10 μM RR and reversed upon washout of FTS. b, current-voltage relationships at time points 1, 2, and 3 from a. The FTS-induced current was outwardly rectifying, with a region of negative slope conductance (c). Similar currents were not observed in untransfected CHO-TREx cells.

channel slope conductance were found to be 79 ± 1 pS (n = 6) (Fig. 6C).

Rat Dorsal Root Ganglion Studies. To determine whether FTS could activate native TRPA1 channels, we studied its effects on cultured rat DRG cells. Because little is known about potential species differences in TRPA1 sensitivity to FTS, we studied the effects of this compound at a single, high concentration of 30 μM. DRG cells studied were small to medium diameter (~30 μm), and they were all capsaicin-sensitive (Fig. 7, A and C). In 5 of 15 cells, 30 μM FTS activated a small, slowly developing, and noisy inward current at a holding potential of −60 mV. A representative example is shown in Fig. 7A. All cells that responded to FTS also responded to 100 μM AITC. Where studied, FTS-induced inward currents were blocked by 10 μM RR (Fig. 7B). Ten of 15 cells were insensitive to 10 μM FTS. These cells were also insensitive to 100 μM AITC (Fig. 7C).

Mechanism of Action. Reversible covalent modification of cysteine residues in the N terminus of TRPA1 is thought to underlie the agonist activity of chemically reactive compounds such as AITC and cinnamaldehyde (Hinman et al., 2006; Macpherson et al., 2007). In particular, the quadruple mutant (TRPA1-M4) containing C621S, C641S, C665S, and K710R (numbering according to NP-015628.1) has been shown previously to be fully functional but completely insensitive to AITC (Hinman et al., 2006). To determine whether a similar mechanism underlies the activity of the novel TRPA1 agonists described above, we studied the effects of these agents on calcium fluorescence in HEK293 cells transiently transfected with TRPA1-M4. HEK293 cells were used for these studies because we were unable to express the mutant channel in the CHO-TREx cell line. We also tested TRPA1 transiently transfected into HEK293 cells, to allow a direct comparison of the wild-type and mutant channels in the same cellular background. Responses were normalized to the response of HEK-TRPA1 to 100 μM FTS. AITC was devoid of activity in the TRPA1-M4-expressing cells (Fig. 8A), confirming the findings of Hinman and colleagues (2006), whereas the activity of disulfiram, chlordantoin, and 15d-PGJ_2 was substantially reduced (Table 2). In contrast, and as illustrated in Fig. 8B, FTS retained the ability to increase fluorescence in TRPA1-M4-transfected cells, albeit at reduced potency compared with the effects seen in HEK-TRPA1 cells. Similar results were obtained with FTA (Table 2). Whole-cell electrophysiological experiments were conducted to confirm the activity of FTS on the TRPA1-M4 mutant channels, in the same way as described above for the wild-type channel. The results of a representative experiment are shown in Fig. 8C. FTS was without effect at 1 μM but elicited an inward current at concentrations of 3 and 10 μM. FTS-induced currents were generally smaller than those measured in CHO-TREx-TRPA1 cells, but the threshold FTS concentration for activation of TRPA1-M4 was identical to that determined for activation of TRPA1 (compare Fig. 4 and 8C). The whole-cell currents activated by FTS in TRPA1-M4 expressing cells were blocked by 10 μM RR (data not shown). ETYA also increased calcium fluorescence in cells expressing TRPA1-M4. However, the concentrations required for activity in the transiently transfected HEK293 cells were similar to those that caused increases in fluorescence in HEK-WT. Hence, it is not clear whether this compound activates TRPA1-M4.

Discussion

In this study, we have identified several TRPA1 agonists. These agents include several lipid compounds (farnesyl thiosalicylic acid, farnesyl thioacetic acid, and 15-deoxy-$\Delta^{12,14}$-prostaglandin J_2), disulfiram, and the antifungal agent chlordantoin.

Of the TRPA1 agonists identified, we characterized the effects of FTS in most detail. This compound activated TRPA1 channels in both fluorescent and electrophysiological assays at

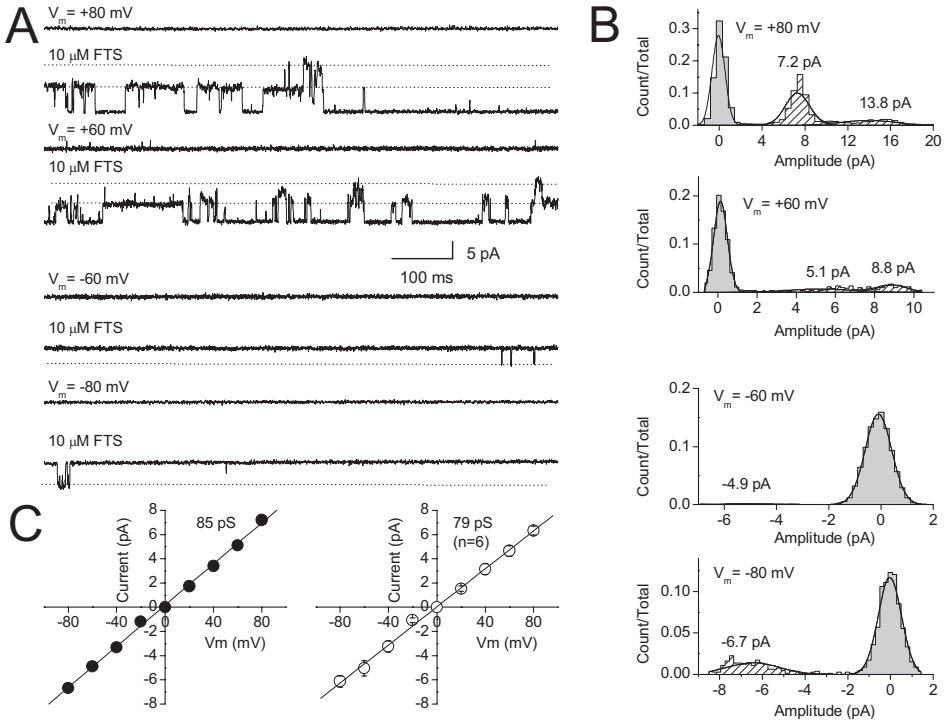

Fig. 6. FTS activates TRPA1 in inside-out patch recordings. A, representative sweeps from an inside-out patch recording at different voltages as indicated. For each voltage, the top trace is recorded before FTS application, and the bottom is recorded after application of 10 μM FTS to the bath (intracellular solution). Dotted lines indicate open states. B, current amplitude histograms at various patch potentials. C, left, plot of the single channel current amplitude (obtained from fitting Gaussian curves to amplitude histograms shown in B against the patch potential for a representative experiment. Linear regression analysis of the data yields a slope conductance of 85 pS. C, right, plot of the mean single channel current amplitude against the patch potential for n = 6 recordings. Linear regression analysis of the data yields a slope conductance of 79 ±1 pS.

concentrations that were devoid of effects on untransfected cells and on related TRP channels. Concentration-response curves for FTS were quite steep in both calcium fluorescence experiments and patch-clamp studies, suggesting there is not a 1:1 relationship between binding and channel activation. The reasons for this are not clear. This could be indicative of some degree of cooperative binding. Alternatively, it may represent a degree of positive feedback as a result of the permeating calcium ions exerting direct effects on TRPA1 (Doerner et al., 2007; Zurborg et al., 2007). The effects of FTS in the fluorescence assay were substantially reduced in the absence of extracellular calcium, indicating that FTS stimulated calcium entry through calcium-permeable TRPA1 channels is primarily responsible for the increased calcium fluorescence observed (rather than intracellular calcium release). The effects of FTS were also inhibited by the nonselective TRP channel blocker RR. The effect of FTS seems to be specific and not a general property of lipophilic farnesyl-containing compounds, because a number of related compounds were either significantly less potent (FTA) or inactive as TRPA1 agonists. Collectively, these findings strongly suggest that FTS represents a novel TRPA1 agonist. In contrast to AITC, FTS retained activity on an AITC-insensitive quadruple cysteine/lysine mutant. Although the activity of FTS was slightly lower on the mutant compared with the WT channel in fluorescence studies, we reasoned that this apparent shift in potency might be a consequence of lower expression levels of TRPA1-M4 compared with the wild-type TRPA1 construct. The finding that the threshold FTS concentration for activation of TRPA1-M4 was identical to that determined for activation of TRPA1 in whole-cell electrophysiological studies supports this conclusion. Therefore, studies using the quadruple cysteine/lysine mutant demonstrate that the mechanism of action of FTS differs from that of reactive agents such as AITC. The precise mechanism by which FTS activates TRPA1 remains unclear. FTS is an inhibitor of prenylated protein methyltransferase, an enzyme responsible for methylation of prenylated cysteine of Ras and other prenylated proteins (Marom et al., 1995). TRPA1 agonist activity was also observed with a second methyltransferase inhibitor, FTA (Tan et al., 1991), but not with the structurally related methyltransferase substrate *N*-acetyl-*S*-farnesyl-L-cysteine (Tan et al., 1991). Because some precedent exists for regulation of ion channels by methylation, it is possible that inhibition of a methyltransferase may be involved in TRPA1 activation by FTS (Becchetti et al., 2000;

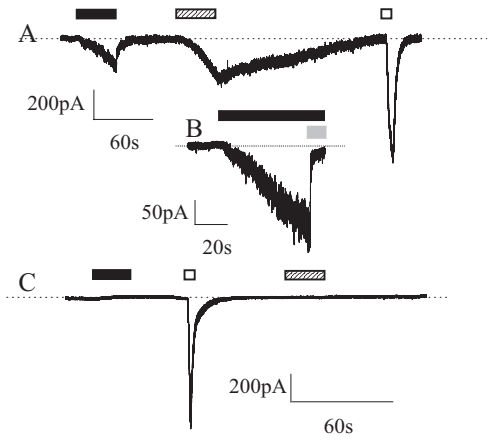

Fig. 7. FTS activates a ruthenium red sensitive current in cultured rat DRG neurons. A, representative whole-cell currents in a DRG neuron. Cells were held at −60 mV. FTS (30 μM) induced a slowly activating inward current. This same cell also responded to 100 μM AITC and to 1 μM capsaicin. B, an expanded view of a 30 μM FTS-induced current in a second DRG cell. Application of 10 μM ruthenium red rapidly blocks the FTS-induced inward current. C, a different DRG neuron, sensitive to capsaicin but not to AITC, is also unresponsive to FTS. Solid bar, FTS (30 μM); hatched bar, AITC (100 μM); open bar, capsaicin (1 μM); gray bar, RR (10 μM).

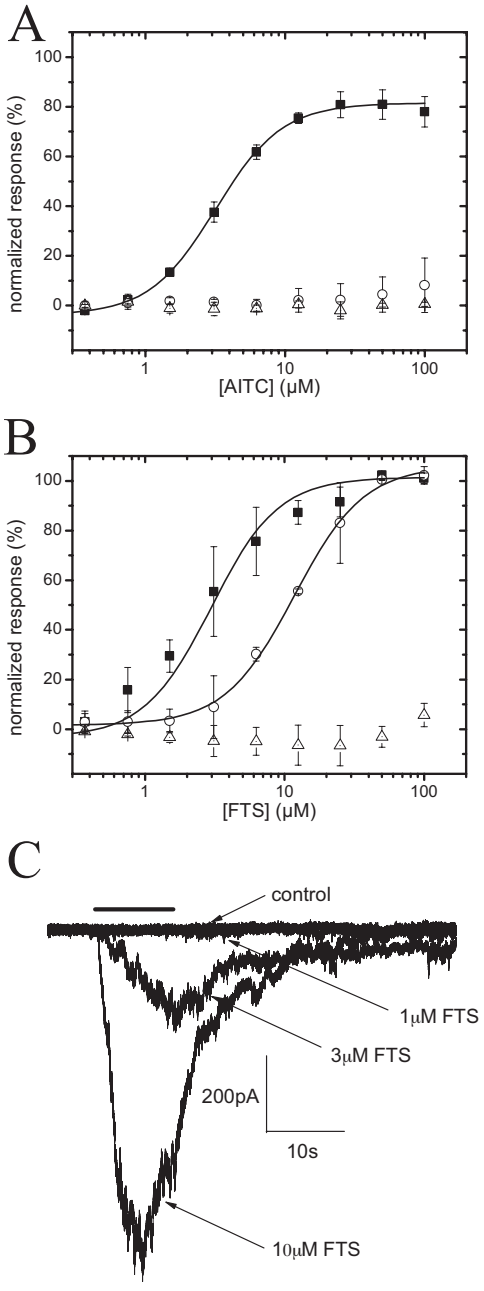

Fig. 8. Effect of TRPA1 agonists on TRPA1-M4. Concentration-response curves for agonists were determined in the FLIPR assay. Cells were transiently transfected with either WT-TRPA1 (■) or TRPA1-M4 (○). Responses were compared with the effects of agonists in untransfected HEK293 cells (△). Error bars represent the S.D. of three independent experiments. Data were normalized to the response to 100 μM FTS. Solid lines are Hill fits to the data. A, AITC. B, FTS. C, concentration-dependent activation of human TRPA-M4 by farnesyl thiosalicylic acid in a whole-cell patch-clamp experiment. Increasing concentrations of FTS were applied to a TRPA1-M4 expressing cell at a holding potential of −60 mV, with washout between each concentration. The threshold concentration for activation of TRPA1-M4 was ~3 μM, which is the same as the threshold concentration for activation of WT-TRPA1.

Chen et al., 2004). However, a simpler explanation for our findings is that FTS binds to TRPA1 to directly activate the channel, in a manner analogous to capsaicin-induced activation TRPV1. A direct effect on TRPA1 is supported by the demonstration of TRPA1 agonist activity in excised membrane patches. Although TRPA1 channel activity is generally low in excised patches, as recently described by Kim and Cavanaugh (2007), we found that FTS can stimulate residual TRPA1 activity in inside-out patches. This observation suggests that FTS does not require the presence of diffusible intracellular factors for its activity. Because our recording solutions were calcium free, these patch-clamp studies also rule out the involvement of calcium in the actions of FTS.

In addition to activating recombinant human TRPA1, FTS also induced an inward current in approximately one third of capsaicin-sensitive rat DRG neurons. Cells that were FTS-sensitive were also AITC sensitive. The proportion of cells activated by FTS in our study is similar to that activated by TRPA1 agonists, such as AITC, formalin, 4-hydoxy-2-nonenal, and 15d-PGJ_2 in other studies (Jordt et al., 2004; McNamara et al., 2007; Trevisani et al., 2007; Taylor-Clark et al., 2008). Our findings are also consistent with molecular studies that show TRPA1 expression in a subpopulation of TRPV1-positive sensory ganglion cells. For example, Story et al. (2003) have found that TRPA1 is expressed in approximately 30% of TRPV1-positive DRG cells.

As a TRPA1 agonist with a potentially novel mechanism of action, FTS may be useful in the study of TRPA1 channels. For example, it will be particularly interesting to define the nature of the FTS binding site on the TRPA1 channel and to understand how drug binding can influence channel activity. In addition, because the identity of the pathophysiologically relevant TRPA1 agonist(s) in the setting of inflammation is unclear, the availability of surrogate agonists acting via different sites and mechanisms should increase the likelihood of identifying antagonists with efficacy under pathophysiologically relevant conditions.

The two other lipid-based TRPA1 activators identified in this study were 15d-PGJ_2 and ETYA. Our data show that 15d-PGJ_2 can activate TRPA1 at low micromolar concentrations. The effects of 15d-PGJ_2 are substantially reduced in the TRPA1-M4 mutant, suggesting that this prostaglandin may activate TRPA1 via a similar mechanism to AITC. This conclusion is supported by a recent report showing that TRPA1 activation is also observed with other electrophilic A- and J-series prostaglandins, but not by their nonelectrophilic precursors, PGE2, PGD2, or PGB2 (Taylor-Clark et al., 2007). Our findings and the findings of Taylor-Clark and colleagues suggest that reactive prostanoids may be able to directly activate sensory neurons via a TRPA1-dependent mechanism. ETYA, a somewhat related structure to 15d-PGJ_2, has previously been shown to be a TRPA1 agonist (Bandell et al., 2004). Although our studies confirm this observation to some extent, this compound increases calcium fluorescence in WT-CHO cells, suggesting that ETYA can activate both TRPA1-dependent and TRPA1-independent calcium-mobilizing mechanisms.

Our work also identified two nonlipid TRPA1 agonists. Disulfiram (Antabuse) is an irreversible inhibitor of aldehyde dehydrogenase used in the aversion therapy of recovering alcoholics. Inhibition of this enzyme results in elevated levels of acetaldehyde on alcohol ingestion, leading to acute sensitivity to alcohol, characterized by a series of unpleasant physical responses including nausea, vomiting, headache, skin flushing, and tachycardia. Disulfiram inhibits aldehyde dehydrogenase by inducing the formation of an intramolecular disulfide bridge involving key cysteine residues in the enzyme active site (Lipsky et al., 2001). The inability of disulfiram to activate the TRPA1-M4 mutant channel suggests that modification of critical cysteine residues may also underlie the TRPA1 agonist activity of this compound. Whether the TRPA1 agonist activity contributes to the alcohol-sensitizing effects of disulfiram in any way is unclear.

The final TRPA1 agonist identified in the present study is chlordantoin [5-(1-ethylamyl)3-trichloromethyl thiohydantoin; Sporostacin], a topical antifungal agent. Although chemically distinct, chlordantoin, like AITC and cinnamaldehyde, is electrophilic and it would be expected to react with the free thiol of a cysteine residue. Given its chemical nature, it is not surprising that this compound is without effect on the TRPA1-M4 mutant.

In summary, we have used a combination of calcium fluorescent assays and whole-cell electrophysiology to identify several TRPA1 agonists, including several lipid compounds (farnesyl thiosalicylic acid, farnesyl thioacetic acid, and 15d-prostaglandin J_2), disulfiram, and chlordantoin. These agents may help in understanding the molecular pharmacology of TRPA1 that may ultimately facilitate the identification of novel analgesic agents.

TABLE 2

Summary of the activity of TRPA1 agonists in HEK293 cells transiently expressing TRPA1 and TRPA1-M4, and in untransfected cells

Values are the mean ± S.D. of nonlinear least-squares fit parameters for $n = 3$ to 5 concentration-response experiments. Maximal response is the ratio of the high-concentration response relative to the response of HEK293-TRPA1 to 100 μM FTS.

Agonist	TRPA1		TRPA1 Mutant		HEK-WT	
	EC_{50}	Maximal Response	EC_{50}	Maximal Response	EC_{50}	Maximal Response
	μM		μM		μM	
AITC	5 ± 2	0.77	—	—	—	—
FTS	7 ± 4	1.3 ± 0.1	11 ± 5	0.95 ± 0.04	—	—
FTA	100 ± 40	1.0 ± 0.1	160 ± 40	0.9 ± 0.2	—	—
Disulfiram	3 ± 2	0.8 ± 0.1	—	—	—	—
Chlordantoin	3 ± 1	0.9 ± 0.1	30 ± 10	0.43 ± 0.07	—	—
15d-PGJ_2	22 ± 7	1.2 ± 0.1	210 ± 70	1.2 ± 0.2	300[a]	N.D.
ETYA	4[a]	N.D.	25[a]	N.D.	25[a]	N.D.

—, <20% response at the highest concentration tested; N.D., not determined.

[a] Could not be fit accurately with a Hill function. Instead of an EC_{50} value, the threshold concentration (i.e., the average concentration required to increase the normalized response by 20%) is provided for this compound.

Acknowledgments

We acknowledge the valuable assistance of Dr. Chao-Feng Zheng (Biomyx Technology, San Diego, CA) for generating the TRPA1 cell line and the TRPA1-M4 mutant. We are also grateful to our colleagues Drs. Yi Lui and Ning Qin for providing the TRPV2 and TRPM8 cell lines.

References

Andersson DA, Chase HW, and Bevan S (2004) TRPM8 activation by menthol, icilin, and cold is differentially modulated by intracellular pH. *J Neurosci* **24:**5364–5369.

Bandell M, Story GM, Hwang SW, Viswanath V, Eid SR, Petrus MJ, Earley TJ, and Patapoutian A (2004) Noxious cold ion channel TRPA1 is activated by pungent compounds and bradykinin. *Neuron* **41:**849–857.

Bautista DM, Jordt SE, Nikai T, Tsuruda PR, Read AJ, Poblete J, Yamoah EN, Basbaum AI, and Julius D (2006) TRPA1 mediates the inflammatory actions of environmental irritants and proalgesic agents. *Cell* **124:**1269–1282.

Bautista DM, Movahed P, Hinman A, Axelsson HE, Sterner O, Hogestatt ED, Julius D, Jordt SE, and Zygmunt PM (2005) Pungent products from garlic activate the sensory ion channel TRPA1. *Proc Natl Acad Sci U S A* **102:**12248–12252.

Becchetti A, Kemendy AE, Stockand JD, Sariban-Sohraby S, and Eaton DC (2000) Methylation increases the open probability of the epithelial sodium channel in A6 epithelia. *J Biol Chem* **275:**16550–16559.

Chen YF, Zhang AY, Zou AP, Campbell WB, and Li PL (2004) Protein methylation activates reconstituted ryanodine receptor-ca release channels from coronary artery myocytes. *J Vasc Res* **41:**229–240.

Corey DP, Garcia-Anoveros J, Holt JR, Kwan KY, Lin SY, Vollrath MA, Amalfitano A, Cheung EL, Derfler BH, Duggan A, et al. (2004) TRPA1 is a candidate for the mechanosensitive transduction channel of vertebrate hair cells. *Nature* **432:**723–730.

Diogenes A, Akopian AN, and Hargreaves KM (2007) NGF up-regulates TRPA1: implications for orofacial pain. *J Dent Res* **86:**550–555.

Doerner JF, Gisselmann G, Hatt H, and Wetzel CH (2007) Transient receptor potential channel A1 is directly gated by calcium ions. *J Biol Chem* **282:**13180–13189.

Frederick J, Buck ME, Matson DJ, and Cortright DN (2007) Increased TRPA1, TRPM8, and TRPV2 expression in dorsal root ganglia by nerve injury. *Biochem Biophys Res Commun* **358:**1058–1064.

Fujita F, Moriyama T, Higashi T, Shima A, and Tominaga M (2007) Methyl p-hydroxybenzoate causes pain sensation through activation of TRPA1 channels. *Br J Pharmacol* **151:**153–160.

Hinman A, Chuang HH, Bautista DM, and Julius D (2006) TRP channel activation by reversible covalent modification. *Proc Natl Acad Sci U S A* **103:**19564–19568.

Hu HZ, Gu Q, Wang C, Colton CK, Tang J, Kinoshita-Kawada M, Lee LY, Wood JD, and Zhu MX (2004) 2-aminoethoxydiphenyl borate is a common activator of TRPV1, TRPV2, and TRPV3. *J Biol Chem* **279:**35741–35748.

Jaquemar D, Schenker T, and Trueb B (1999) An ankyrin-like protein with transmembrane domains is specifically lost after oncogenic transformation of human fibroblasts. *J Biol Chem* **274:**7325–7333.

Jeske NA, Patwardhan AM, Gamper N, Price TJ, Akopian AN, and Hargreaves KM (2006) Cannabinoid WIN 55,212–2 regulates TRPV1 phosphorylation in sensory neurons. *J Biol Chem* **281:**32879–32890.

Jordt SE, Bautista DM, Chuang HH, McKemy DD, Zygmunt PM, Hogestatt ED, Meng ID, and Julius D (2004) Mustard oils and cannabinoids excite sensory nerve fibres through the TRP channel ANKTM1. *Nature* **427:**260–265.

Kim D and Cavanaugh EJ (2007) Requirement of a soluble intracellular factor for activation of transient receptor potential A1 by pungent chemicals: role of inorganic polyphosphates. *J Neurosci* **27:**6500–6509.

Kwan KY, Allchorne AJ, Vollrath MA, Christensen AP, Zhang DS, Woolf CJ, and Corey DP (2006) TRPA1 contributes to cold, mechanical, and chemical nociception but is not essential for hair-cell transduction. *Neuron* **50:**277–289.

Lipsky JJ, Shen ML, and Naylor S (2001) Overview–in vitro inhibition of aldehyde dehydrogenase by disulfiram and metabolites. *Chem Biol Interact* **130-132:**81–91.

Liu Y, Lubin ML, Reitz TL, Wang Y, Colburn RW, Flores CM, and Qin N (2006) Molecular identification and functional characterization of a temperature-sensitive transient receptor potential channel (TRPM8) from canine. *Eur J Pharmacol* **530:**23–32.

Macpherson LJ, Dubin AE, Evans MJ, Marr F, Schultz PG, Cravatt BF, and Patapoutian A (2007) Noxious compounds activate TRPA1 ion channels through covalent modification of cysteines. *Nature* **445:**541–545.

Marom M, Haklai R, Ben-Baruch G, Marciano D, Egozi Y, and Kloog Y (1995) Selective inhibition of Ras-dependent cell growth by farnesylthiosalisylic acid. *J Biol Chem* **270:**22263–22270.

McNamara CR, Mandel-Brehm J, Bautista DM, Siemens J, Deranian KL, Zhao M, Hayward NJ, Chong JA, Julius D, Moran MM, et al. (2007) TRPA1 mediates formalin-induced pain. *Proc Natl Acad Sci U S A* **104:**13525–13530.

Nagata K, Duggan A, Kumar G, and Garcia-Anoveros J (2005) Nociceptor and hair cell transducer properties of TRPA1, a channel for pain and hearing. *J Neurosci* **25:**4052–4061.

Namer B, Seifert F, Handwerker HO, and Maihofner C (2005) TRPA1 and TRPM8 activation in humans: effects of cinnamaldehyde and menthol. *Neuroreport* **16:**955–959.

Neeper MP, Liu Y, Hutchinson TL, Wang Y, Flores CM, and Qin N (2007) Activation properties of heterologously expressed mammalian TRPV2: evidence for species dependence. *J Biol Chem* **282:**15894–15902.

Niforatos W, Zhang XF, Lake MR, Walter KA, Neelands T, Holzman TF, Scott VE, Faltynek CR, Moreland RB, and Chen J (2007) Activation of TRPA1 channels by the fatty acid amide hydrolase inhibitor 3′-carbamoylbiphenyl-3-yl cyclohexylcarbamate (URB597). *Mol Pharmacol* **71:**1209–1216.

Nilius B, Watanabe H, and Vriens J (2003) The TRPV4 channel: structure-function relationship and promiscuous gating behaviour. *Pflugers Arch* **446:**298–303.

Obata K, Katsura H, Mizushima T, Yamanaka H, Kobayashi K, Dai Y, Fukuoka T, Tokunaga A, Tominaga M, and Noguchi K (2005) TRPA1 induced in sensory neurons contributes to cold hyperalgesia after inflammation and nerve injury. *J Clin Invest* **115:**2393–2401.

Stokes A, Wakano C, Koblan-Huberson M, Adra CN, Fleig A, and Turner H (2006) TRPA1 is a substrate for de-ubiquitination by the tumor suppressor CYLD. *Cell Signal* **18:**1584–1594.

Story GM, Peier AM, Reeve AJ, Eid SR, Mosbacher J, Hricik TR, Earley TJ, Hergarden AC, Andersson DA, Hwang SW, et al. (2003) ANKTM1, a TRP-like channel expressed in nociceptive neurons, is activated by cold temperatures. *Cell* **112:**819–829.

Tan EW, Perez-Sala D, Canada FJ, and Rando RR (1991) Identifying the recognition unit for G protein methylation. *J Biol Chem* **266:**10719–10722.

Taylor-Clark TE, Undem BJ, Macglashan DW Jr, Ghatta S, Carr MJ, and McAlexander MA (2008) Prostaglandin-induced activation of nociceptive neurons via direct interaction with transient receptor potential A1 (TRPA1). *Mol Pharmacol* **73:**274–281.

Trevisani M, Siemens J, Materazzi S, Bautista DM, Nassini R, Campi B, Imamachi N, Andre E, Patacchini R, Cottrell GS, et al. (2007) 4-Hydroxynonenal, an endogenous aldehyde, causes pain and neurogenic inflammation through activation of the irritant receptor TRPA1. *Proc Natl Acad Sci U S A* **104:**13519–13524.

Zurborg S, Yurgionas B, Jira JA, Caspani O, and Heppenstall PA (2007) Direct activation of the ion channel TRPA1 by Ca^{2+}. *Nat Neurosci* **10:**277–279.

Address correspondence to: Dr. Alan D. Wickenden, Johnson & Johnson Pharmaceutical Research & Development, L.L.C., 3210 Merryfield Row, San Diego, CA 92121. E-mail: awickend@prdus.jnj.com